



UNIVERSITÉ DE  
MONTPELLIER

MIMESIS

$\phi$ -FEM-FNO: A NEW APPROACH TO TRAIN A NEURAL OPERATOR  
AS A FAST PDE SOLVER FOR VARIABLE GEOMETRIES.

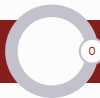
28/05/2024

CANUM 2024, Le Bois-Plage-en-Ré, Ile de Ré

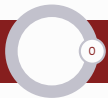
M. Duprez<sup>1</sup>, V. Lleras<sup>2</sup>, A. Lozinski<sup>3</sup>, V. Vigon<sup>4</sup> and **K. Vuillemot**<sup>1,2</sup>

<sup>1</sup>Inria, Strasbourg, France, <sup>2</sup>IMAG, Montpellier, France,

<sup>3</sup>LMB, Besançon, France, <sup>4</sup>IRMA, Strasbourg, France.



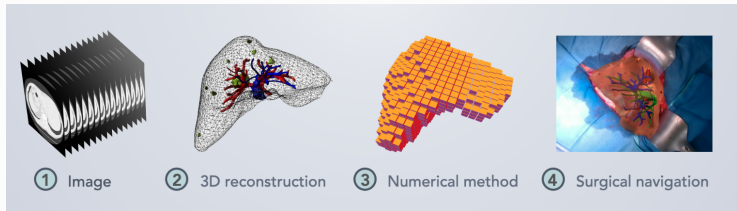
- 1 Motivation
- 2 The  $\phi$ -FEM technique
- 3  $\phi$ -FEM and Neural networks
- 4 Conclusion



- 1 Motivation
- 2 The  $\phi$ -FEM technique
- 3  $\phi$ -FEM and Neural networks
- 4 Conclusion

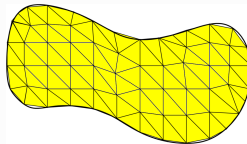
## Objectives

Develop **real-time, patient specific digital twins** for computer-aided surgical interventions.

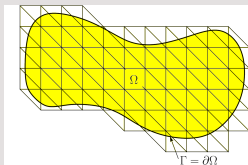


- ▶ Simulation of the deformations of organs : PDEs  $\rightarrow$  FEMs,
- ▶ Complex geometries  $\rightarrow$  Unfitted FEMs,
- ▶ Real-time constructions  $\rightarrow$  machine learning techniques.

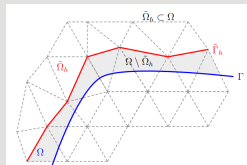
New method :  $\phi$ -FEM, unfitted method, precise, easy to implement.



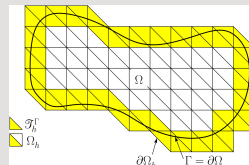
(a) Standard FEM (Clough 60s).



(b) XFEM (Moes and al., 2006)  
 → Non-classical shape functions,  
 CutFEM (Burman, Hansbo, 2010-2014)  
 → cut cells and partial integrals.



(c) Shifted Boundary method (Main, Scovazzi, 2017)  
 → Taylor development near the boundary.



(d)  $\phi$ -FEM (Duprez and Lozinski, 2020)  
 → Level-set function

Problems on complex shapes → unfitted FEMs



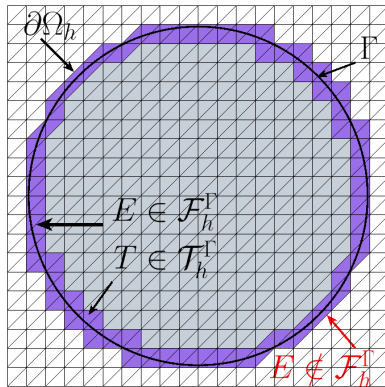
- 1 Motivation
- 2 The  $\phi$ -FEM technique**
- 3  $\phi$ -FEM and Neural networks
- 4 Conclusion

## Level-set function

$$\Omega = \{\phi < 0\} \text{ and } \Gamma = \{\phi = 0\}.$$

## The spaces

- ▶  $\mathcal{T}_h$  :  $\phi$ -FEM mesh,
- ▶  $\mathcal{T}_h^\Gamma$  : cells of  $\mathcal{T}_h$  cut by the boundary (purple triangles),
- ▶  $\mathcal{F}_h^\Gamma$  : internal facets of  $\mathcal{T}_h^\Gamma$ .



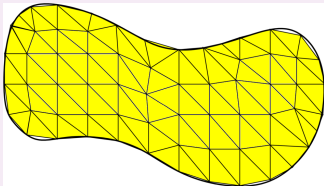
Example with  $\phi(x, y) = -1 + x^2 + y^2$ .

## Example (Poisson-Dirichlet equation)

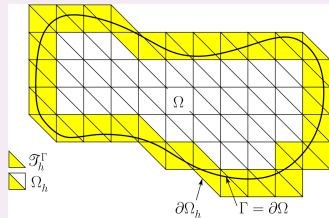
$$-\Delta u = f \quad \text{in } \Omega, \quad u = g \quad \text{on } \Gamma.$$

**Standard FEM**

$$\text{Find } u \text{ s.t. } \begin{cases} -\Delta u = f, & \text{in } \Omega, \\ u = g, & \text{on } \Gamma. \end{cases}$$

 **$\phi$ -FEM**

$$\text{Find } w \text{ s.t. } \begin{cases} -\Delta u = f, & \text{in } \Omega_h, \\ u = \phi w + g, & \text{in } \Omega_h. \end{cases}$$





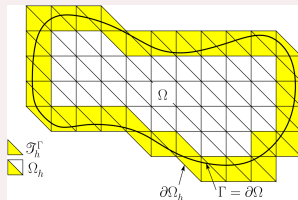
Example (Poisson-Dirichlet equation)

$$-\Delta u = f \quad \text{in } \Omega, \quad u = g \quad \text{on } \Gamma.$$

$\phi$ -FEM scheme

Find  $w_h$  such that for all  $v_h$ ,

$$\begin{aligned} & \int_{\Omega_h} \nabla(\phi_h w_h + g_h) \cdot \nabla(\phi_h v_h) \\ & - \int_{\partial\Omega_h} \frac{\partial}{\partial n}(\phi_h w_h + g_h) \phi_h v_h \\ & + \text{stabs} = \int_{\Omega_h} f_h \phi_h v_h - \text{stabs} . \end{aligned}$$



## Who are «stabs»?

- ▶ First order : Ghost penalty ( $\mathcal{S}_1$ ),
- ▶ Second order : least square imposition of the strong formulation on  $\mathcal{T}_h^\Gamma$  ( $\mathcal{S}_2$ ).

$$\begin{aligned}
 & \int_{\Omega_h} \nabla(\phi_h w_h + g_h) \cdot \nabla(\phi_h v_h) - \int_{\partial\Omega_h} \frac{\partial}{\partial n}(\phi_h w_h + g_h) \phi_h v_h \\
 & \quad + \underbrace{\sigma h \sum_{E \in \mathcal{F}_\Gamma} \int_E \left[ \frac{\partial}{\partial n}(\phi_h w_h + g_h) \right] \left[ \frac{\partial}{\partial n}(\phi_h v_h) \right]}_{(\mathcal{S}_1) : \text{Ghost penalty, jump over the facets}} \\
 & \quad + \underbrace{\sigma h^2 \sum_{T \in \mathcal{T}_h^\Gamma} \int_T \Delta(\phi_h w_h + g_h) \Delta(\phi_h w_h)}_{(\mathcal{S}_2) : \text{least square imposition of the governing equation}} = \int_{\Omega_h} f_h \phi_h v_h \\
 & \quad \underbrace{- \sigma h^2 \sum_{T \in \mathcal{T}_h^\Gamma} \int_T f \Delta(\phi_h w_h)}_{\mathcal{S}_2\text{'s friend}} .
 \end{aligned}$$

## Interests of the method

- ▶ Optimal convergence in  $L^2$  and  $H^1$  norms,
- ▶ **Easy to implement**: standard shape functions, no cut cells  $\rightarrow$  standard quadrature rules,
- ▶ Acceptable conditioning of the finite element matrix,
- ▶ **No need to generate a conforming mesh.**

## Other schemes

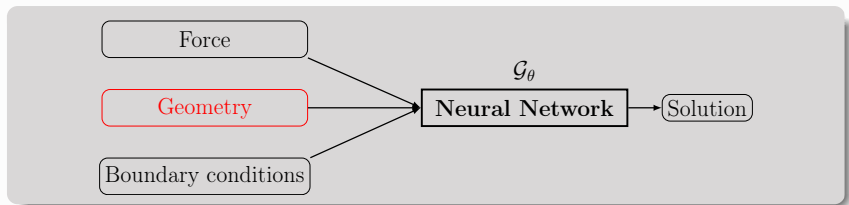
- ▶ Dirichlet or Neumann boundary conditions,
- ▶ Linear elasticity problems,
- ▶ Stokes problem,
- ▶ Heat equation.



- 1 Motivation
- 2 The  $\phi$ -FEM technique
- 3  $\phi$ -FEM and Neural networks
- 4 Conclusion

In the context of real-time simulations, we need  
**quasi-instantaneous results.**

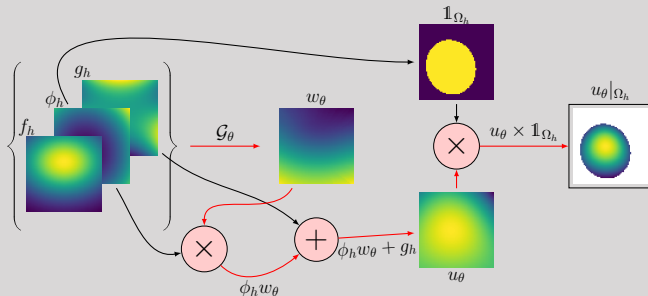
- ▶  $\phi$ -FEM : precise but slow  $\rightarrow$  Not real-time
- ▶ Neural Networks  $\rightarrow$  Real time
- ▶  $\phi$ -FEM + Neural Networks  $\rightarrow$  Precise and real-time method?



In the context of real-time simulations, we need  
**quasi-instantaneous results.**

- ▶  $\phi$ -FEM : precise but slow  $\rightarrow$  Not real-time
- ▶ Neural Networks  $\rightarrow$  Real time
- ▶  $\phi$ -FEM + Neural Networks  $\rightarrow$  Precise and real-time method?

The idea : construct an operator  $\mathcal{G}_\theta$



How to combine  $\phi$ -FEM and neural networks to obtain fast and precise results?

—→ the Fourier Neural Operator.

### Why choose the FNO?

- ▶ Neural operator : learns a mapping, not a solution,
- ▶ Uses FFT —→ requires Cartesian grid, as  $\phi$ -FEM does,
- ▶ According to the authors, more accurate than other ML-methods :

	NN	PCANN	DeepOnet	GNO	LNO	FNO
Darcy Flow	0.17	0.02	0.04	0.03	0.05	<b>0.01</b>
1D Burgers	0.47	0.04	0.06	0.06	0.02	<b>0.001</b>

$L^2$  errors of different methods [Kovachki et al, 2023].

- ▶ Almost no need to change the underlying architecture when changing the governing PDE.

Parametric application :

$$\mathcal{G}_\theta : \mathbb{R}^{n_x \times n_y \times 3} \xrightarrow{N} \mathbb{R}^{n_x \times n_y \times 3} \xrightarrow{P_\theta} \mathbb{R}^{n_x \times n_y \times n_d} \xrightarrow{\mathcal{H}_\theta^1} \mathbb{R}^{n_x \times n_y \times n_d} \xrightarrow{\mathcal{H}_\theta^2} \dots \xrightarrow{\mathcal{H}_\theta^4} \mathbb{R}^{n_x \times n_y \times n_d} \xrightarrow{Q_\theta} \mathbb{R}^{n_x \times n_y \times 1} \xrightarrow{N^{-1}} \mathbb{R}^{n_x \times n_y \times 1} .$$

- ▶ In and out dimensions :  $X = (f_h, \phi_h, g_h) \rightarrow w_h$ , with  $f_h, \phi_h, g_h$  and  $w_h$  images of shape  $(n_x, n_y)$ .
- ▶  $N$  and  $N^{-1}$  : standardization and unstandardization (channel by channel),
- ▶  $P_\theta$  and  $Q_\theta$  : «embedding and projection»,

$$P_\theta(X)_{ijk} = \sum_{k'=1}^3 W_{kk'}^{P_\theta} X_{ijk'} + B_k^{P_\theta} \in \mathbb{R}^{n_d} ,$$

→ from original dimension 3 to «hidden dimension»,  $n_d \gg 3$ .

$$Q_\theta(X)_{ij} = \left[ \sum_{k=1}^{n_d} W_{1k}^{Q_\theta, 2} \sigma \left( \sum_{k'=1}^{n_d} W_{kk'}^{Q_\theta, 1} X_{ijk'} + B_k^{Q_\theta, 1} \right) \right] + B^{Q_\theta, 2} \in \mathbb{R}$$

→ from «hidden dimension»  $n_d$  to final dimension 1.

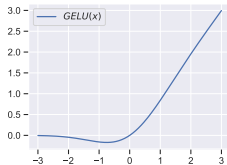


Parametric application :

$$\begin{aligned}
 \mathcal{G}_\theta : \mathbb{R}^{n_x \times n_y \times 3} \xrightarrow{N} \mathbb{R}^{n_x \times n_y \times 3} \xrightarrow{P_\theta} \mathbb{R}^{n_x \times n_y \times n_d} \xrightarrow{\mathcal{H}_\theta^1} \mathbb{R}^{n_x \times n_y \times n_d} \xrightarrow{\mathcal{H}_\theta^2} \\
 \dots \xrightarrow{\mathcal{H}_\theta^4} \mathbb{R}^{n_x \times n_y \times n_d} \xrightarrow{Q_\theta} \mathbb{R}^{n_x \times n_y \times 1} \xrightarrow{N^{-1}} \mathbb{R}^{n_x \times n_y \times 1} .
 \end{aligned}$$

Each layer  $\mathcal{H}_\theta^\ell$  is defined by :

$$\mathcal{H}_\theta^\ell = \sigma \left( \begin{array}{ccc} & \mathcal{C}_\theta^\ell(X) & + \\ & \downarrow & \\ & \mathcal{F}^{-1} \left( W^{C_\theta^\ell} \mathcal{F}(X) \right) & + \\ & \downarrow & \\ & \text{with } \mathcal{F} \text{ the real-FFT and} & \\ & \mathcal{F}^{-1} \text{ its inverse.} & \\ & \downarrow & \\ & \text{The coefficients of } W^{C_\theta^\ell} & \\ & \text{are complex trainable} & \\ & \text{parameters.} & \\ & \downarrow & \\ & \mathcal{B}_\theta^\ell(X) & \\ & \downarrow & \\ & \mathcal{B}_\theta^\ell(X)_{ijk} & \\ & = \sum_{k'=1}^{n_d} W_{kk'}^{\mathcal{B}_\theta^\ell} X_{ijk'} + B_k^{\mathcal{B}_\theta^\ell} & \\ & \downarrow & \\ & \text{The coefficients of } W^{\mathcal{B}_\theta^\ell} & \\ & \text{and } B^{\mathcal{B}_\theta^\ell} \text{ are real} & \\ & \text{trainable parameters.} & \end{array} \right)$$



The coefficients of  $W^{C_\theta^\ell}$  are complex trainable parameters.

The coefficients of  $W^{\mathcal{B}_\theta^\ell}$  and  $B^{\mathcal{B}_\theta^\ell}$  are real trainable parameters.

## Question :

How many trainable parameters for  $\phi$ -FEM-FNO?

$$C_{\theta}^l : 2 \times \underbrace{n_d}_{\text{Number of in channels}} \times \underbrace{n_d}_{\text{Number of out channels}} \times \underbrace{m_x \times m_y}_{\text{Number of Fourier modes}}$$

- ▶  $\mathcal{F}(X)$  : RFFT  $\rightarrow$  low frequencies stored in NW and SW corners,
- ▶ High frequencies negligible  $\implies W = 0$  outside NW and SW corners,
- ▶ Size of the corners = «number of modes» =  $m_x, m_y$ ,
- ▶ Finally, for each corner :  $n_d \times n_d \times m_x \times m_y$  parameters  $\rightarrow \times 2$ .

## Total number :

$$P_{\theta} : \underbrace{3 \times n_d + n_d}_{4 \times n_d} + 4 \times \underbrace{\left( 2 \times n_d^2 \times m_x \times m_y + \underbrace{n_d^2 + n_d}_{B_{\theta}^l} \right)}_{\mathcal{H}_{\theta}^l} + \underbrace{Q_{\theta} : n_d \times n_Q + n_Q + n_Q \times 1 + 1}_{(n_d + 2) \times n_Q + 1} .$$

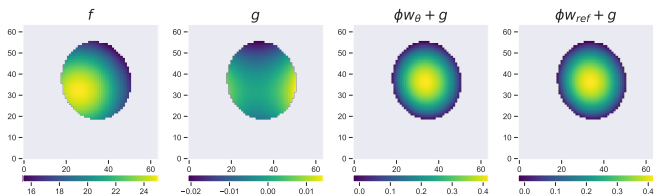
Does not depend on the resolution of the images!

## First test case

$$-\Delta u = f, \text{ in } \Omega, u = g, \text{ on } \Gamma,$$

- ▶  $\Omega$  is a random rotated ellipse defined using the signed distance  $\phi$ ,
- ▶  $f$  is a random gaussian force centered in  $\Omega$  with constant amplitude  
 $\implies f \in [0, 25]$ ,
- ▶  $g_{(\alpha, \beta)}(x, y) = \alpha \left( (x - 0.5)^2 - (y - 0.5)^2 \right) \cos(\beta y \pi)$   
 $\implies g \in [-0.17, 0.15]$ ,
- ▶  $\implies u \in [-0.17, 0.87]$ .

Dataset : 1500 training data, 300 validation data.

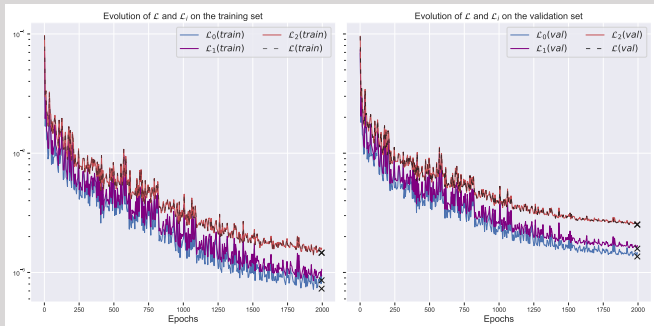


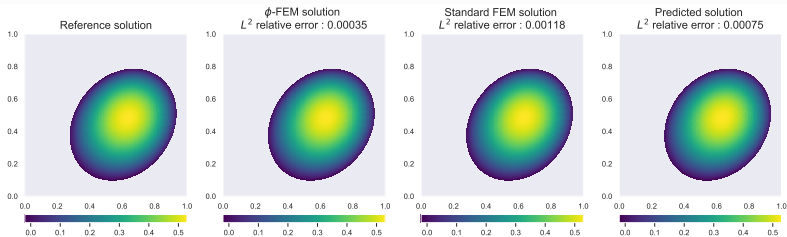
## First test case

$$-\Delta u = f, \text{ in } \Omega, u = g, \text{ on } \Gamma,$$

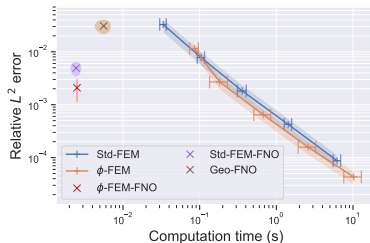
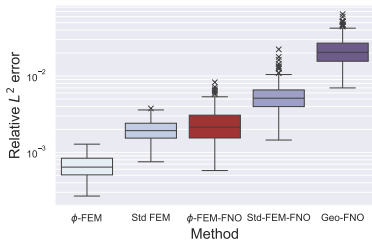
where  $\Omega$  is a random rotated ellipse.

Convergence of the loss function :  $\approx \|\cdot\|_{2, \Omega_h}$





Outputs of the first three methods.



Errors of the methods.

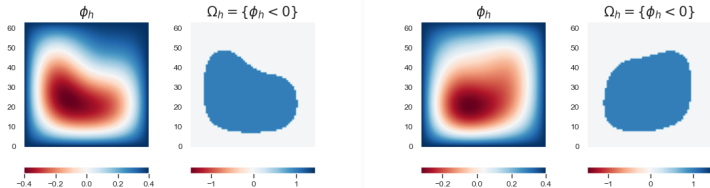
## Second test case

$$-\Delta u = f, \text{ in } \Omega, u = g, \text{ on } \Gamma,$$

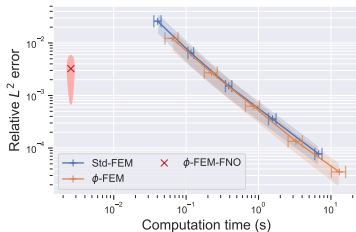
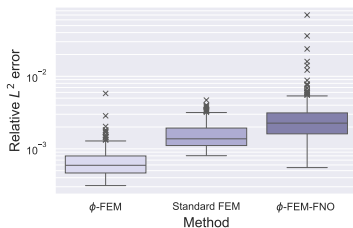
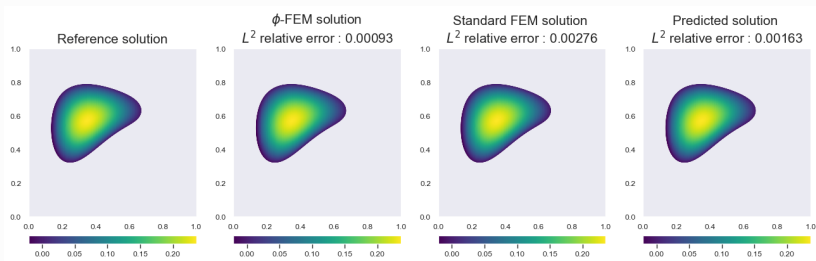
where  $\Omega$  is defined using Fourier series,

$$\phi(x, y) = 0.4 - \sum_{k=1}^3 \sum_{l=1}^3 \alpha_{kl} \sin(k\pi x) \sin(l\pi y),$$

Dataset : 2200 training data, 467 validation data.



Examples of level-set functions and corresponding domains.





- 1 Motivation
- 2 The  $\phi$ -FEM technique
- 3  $\phi$ -FEM and Neural networks
- 4 Conclusion



## Results

- ▶ Real-time :  $\approx 100$  times faster than FEM solvers,
- ▶  $\approx 5$  times faster and more precise than the previous work Geo-FNO.

## Perspectives :

- ▶ More realistic test cases,
- ▶ Mixed Dirichlet-Neumann boundary conditions, Time-Dependant PDE's, Linear and non-linear elasticity, ...
- ▶ 3D problems,
- ▶ Validation on organ geometries.

Thanks for your attention!

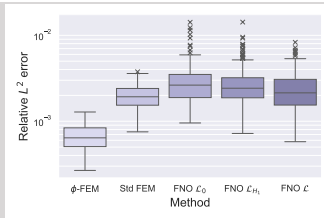
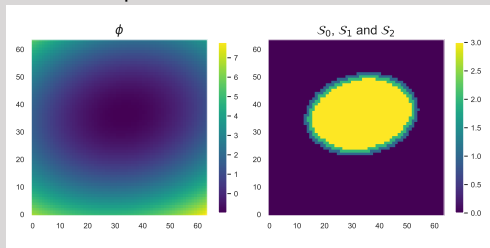
- ▶ The standardization and unstandardization operators are applied channel by channel and are given by :

$$C^N = N(C) = \left( \frac{C - \text{mean}(C^{\text{train}})}{\text{std}(C^{\text{train}})} \right), \quad (N)$$

$$N^{-1}(Y) = Y \times \text{std}(Y^{\text{train}}) + \text{mean}(Y^{\text{train}}). \quad (N^{-1})$$

$$H^2 \text{ norm: } \mathcal{L}^2 \approx \|\cdot\|_{0,S_0}^2 + |\cdot|_{1,S_1}^2 + |\cdot|_{2,S_2}^2$$

- ▶ First and second derivatives : finite differences.
- ▶ Need to reduce the computational domain :



$$\mathcal{L}(U_{\text{true}}; U_{\theta}) = \frac{1}{N_{\text{data}}} \sum_{n=0}^{N_{\text{data}}} \sqrt{\frac{\sum_{i=0}^2 \mathcal{E}_i(u_{\text{true}}^n; u_{\theta}^n)}{\sum_{i=0}^2 \mathcal{N}_i(u_{\text{true}}^n)}},$$

where

$$\mathcal{E}_0(u_{\text{true}}^n; u_{\theta}^n) = \sum_{S_0} \|u_{\text{true}}^n(i, j) - u_{\theta}^n(i, j)\|^2,$$

$$\mathcal{E}_1(u_{\text{true}}^n; u_{\theta}^n) = \sum_{S_1} \left( \|\nabla_x^h u_{\text{true}}^n(i, j) - \nabla_x^h u_{\theta}^n(i, j)\|^2 + \|\nabla_y^h u_{\text{true}}^n(i, j) - \nabla_y^h u_{\theta}^n(i, j)\|^2 \right),$$

$$\mathcal{E}_2(u_{\text{true}}^n; u_{\theta}^n) = \sum_{S_2} \left( \|\nabla_x^h \nabla_x^h u_{\text{true}}^n(i, j) - \nabla_x^h \nabla_x^h u_{\theta}^n(i, j)\|^2 \right.$$

$$\left. + \|\nabla_x^h \nabla_y^h u_{\text{true}}^n(i, j) - \nabla_x^h \nabla_y^h u_{\theta}^n(i, j)\|^2 + \|\nabla_y^h \nabla_y^h u_{\text{true}}^n(i, j) - \nabla_y^h \nabla_y^h u_{\theta}^n(i, j)\|^2 \right),$$

and

$$\mathcal{N}_0(u_{\text{true}}^n) = \sum_{S_0} \|u_{\text{true}}^n(i, j)\|^2,$$

$$\mathcal{N}_1(u_{\text{true}}^n) = \sum_{S_1} \left( \|\nabla_x^h u_{\text{true}}^n(i, j)\|^2 + \|\nabla_y^h u_{\text{true}}^n(i, j)\|^2 \right),$$

$$\mathcal{N}_2(u_{\text{true}}^n) = \sum_{S_2} \left( \|\nabla_x^h \nabla_x^h u_{\text{true}}^n(i, j)\|^2 + \|\nabla_x^h \nabla_y^h u_{\text{true}}^n(i, j)\|^2 + \|\nabla_y^h \nabla_y^h u_{\text{true}}^n(i, j)\|^2 \right).$$